

Effect of Transition of Mounted Chisel Plow from Operation to Transport on Longitudinal Stability of Tractor (Part I- Modeling)

Iman AHMADI (✉)

Summary

In order to investigate the effect of transition of mounted implements from operation to transport on longitudinal stability of a tractor that works on sloping land, a mathematical model was developed. In this model two operation modes for a mounted chisel plow were considered: penetration of the plow into the soil and depth reduction of it, and the effects of transferred forces and torques from the plow on longitudinal stability index of tractor were studied. Longitudinal stability index of tractor was defined as the ratio of the dynamic load of tractor front axle to the static load of it when tractor is on level ground. To test the model, different geometries and mass specifications of tractor MF285 and chisel plow combination were used as the input parameters of the model. According to the results of this study, during plow penetration into the soil, internal forces of the connecting rods were zero and positive values were obtained for the internal force of the connecting rods during depth reduction of the plow; therefore, connecting rods acted only as pulling beams. Furthermore, when the plow depth was increased, the model predicted the increase of the force exerted on the center of gravity of tractor in X direction; however, the force exerted on the center of gravity of tractor in Z direction was almost not affected by the plow depth and height ratio variations. These results were expected and verified that the assumptions of the model have been rational. Moreover, longitudinal stability index of tractor during plow penetration was approximately constant. However at the moment of transition of the plow from operation to transport, this index was reduced abruptly. Therefore in situations that tractor works on steep slopes, plow transition from operation to transport should be avoided.

Key words

longitudinal stability, mathematical model, tractor and mounted chisel plow combination, transition from operation to transport

Department of Agronomy, Khorasgan (Isfahan) Branch, Islamic Azad University, Isfahan, Iran
✉ e-mail: i_ahmadi_m@yahoo.com

Received: August 26, 2013 | Accepted: January 16, 2014

Introduction

Rollover is one of the main causes of fatalities in the farm tractors. No other machine is identified with hazards of the farming more than the tractor, therefore, rollover prevention is an issue of major importance and the subject has been in focus of attention of several researchers. Mashadi and Nasrolahi (2009) considered four reasons for tractor overturning: operation of tractor on steep side slopes; tractor turning with high forward speed; quick application of power to the rear wheels of tractor, and finally pulling the load with tractor that is not attached to the drawbar of this machine. One of the most important advances in protecting tractor driver in an overturn accident is the invention of tractor rollover protective structure (ROPS). However, some specific farming tasks such as operating with tractor in an orchard, do not allow tractors to be equipped with a ROPS. In an attempt to solve this problem, Silleli et al. (2007) reported: "A chemically deploying anchor mechanism was designed with aim to be used for narrow track orchard and vineyard tractors. The efficiency of the mechanism was tested with a rigid anchor attached to the tractor ROPS. The test results showed that the anchor mechanism increases the clearance zone, reduces the amount of tractor surface area touching the ground and decreases the overturning time." Liu and Ayers (1999) conducted valuable researches about the stability of tractors. To study the effects of dynamic state variables of tractor, such as roll and pitch angles or rates, on the tractor stability over terrains with different slopes, several stability tests using tractors equipped with radio-controlled instruments were carried out. Moreover in another study, development of a site-specific driving safety management and stability mapping system utilizing a tractor stability measuring system, differential global positioning system, geographic information system and video mapping system was conducted (Liu et al, 1999). Although a lot of resources have been expended in the last eight decades on research into tractor stability and dynamics in different countries there are still many tractor accidents. Therefore, research must continue, especially in the area of tractor-implement combinations, since this area has received little attention and the tractor alone is relatively stable (Yisa and Terao, 1995). Derivation of a mathematical model for combination of an off-road vehicle and a heavy implement was carried out in the study of Pota et al. (2007). The model was developed with aim to design a robust controller that will enable the high precision control of the implement trajectory. The developed model was subjected to real conditions, such as ground undulation and uncertainty, sloping terrain, tire slippage, and constrained steering of the tractor. Primarily this work was focused on the demonstration and validation of the trailed vehicle system behavior when the trailing implement is subjected to large drag forces due to ground engagement and the significantly large lateral disturbances that occur in real conditions. In another study conducted by Abu Hamadeh and Al Jalil (2004), theoretical simulation of a tractor-trailer system moving up and down sloping ground under different operating conditions was considered. Furthermore, a computer model was developed in order to predict the effect of trailer loading weight and ground slope angle on tractor stability, traction ability, and drawbar loading. The results of that study showed that the tractor becomes unstable when towing a 3570 kg trailer uphill at 28° slope angle. Insufficient traction occurred at slope angles ranging from 15°

to 18° corresponding to trailer weight of 3750 to 750 kg, and finally the parallel component of drawbar pull reached a maximum value of 17318 N when the trailer was pushing the tractor downhill at 30° slope angle.

In spite of these studies, research on longitudinal stability of tractor and mounted implement combination that works on sloping ground during transition from operation to transport is neglected. Therefore, in this study a mathematical model was developed to formulate longitudinal stability index of tractor as a function of different specifications of tractor and plow. Afterwards, with the aid of this model, effect of transition of plow from operation to transport on tractor stability index was simulated.

Methods

Kinematics of three-point hitch mechanism of tractor

Three-point hitch mechanism is a method utilized to attach implements to the tractor. Implements attached to tractor by means of this mechanism are known as mounted implements. In this method, attachment of the implement mast to the tractor is completed by one upper and two lower arms (Figure 1)

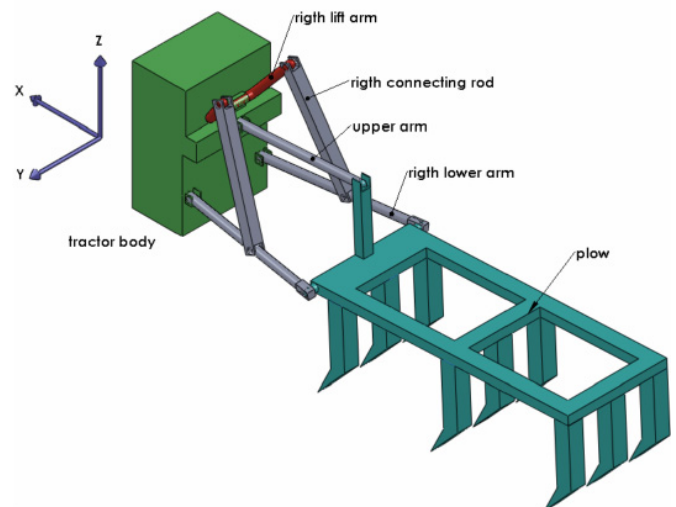


Figure 1. Three-point hitch mechanism of an agricultural tractor

In order to move the implement vertically, hydraulically activated rotation of the lift arms, is exerted on the lower arms by means of two connecting rods. If the pendulum rotation of the arms from left to right is neglected, the three-point hitch mechanism can be considered as a system with one degree of freedom. As shown in Figure 2, the angular position of one arm (for example the angle of the plane of the lower arms with X direction) is sufficient to determine the exact geometry of the system.

According to Figure 2 (b), knowing the angle of lower arms (A_c), angles of the plow (A_p) and upper arm (A_d) can be obtained from equations 1 and 2:

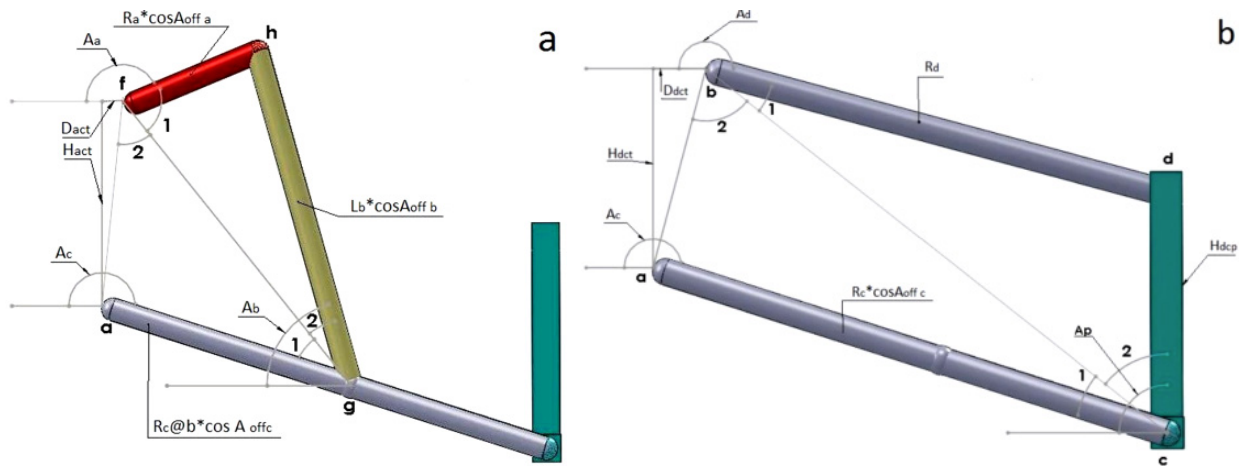


Figure 2. Geometry of lower arm, connecting rod and lift arm (a) and lower arm, plow mast and upper arm (b) in X-Z plane

$$ab = \sqrt{H_{dct}^2 + D_{dct}^2} \quad , \quad \angle bac = \angle A_c - \left(\frac{\pi}{2} + \text{tg}^{-1}\left(\frac{D_{dct}}{H_{dct}}\right)\right)$$

$$\text{cosine law} \rightarrow bc = \sqrt{H_{dct}^2 + D_{dct}^2 + R_c^2 (\cos \angle A_{offc})^2 - 2\sqrt{H_{dct}^2 + D_{dct}^2} R_c (\cos \angle A_{offc}) \sin(\angle A_c - \text{tg}^{-1}\left(\frac{D_{dct}}{H_{dct}}\right))}$$

$$\left\{ \begin{array}{l} \text{sine law} \rightarrow \angle c_1 = \sin^{-1}\left(\frac{ab \cos(\angle A_c - \text{tg}^{-1}\left(\frac{D_{dct}}{H_{dct}}\right))}{bc}\right) \\ \text{cosine law} \rightarrow \angle c_2 = \cos^{-1}\left(\frac{bc^2 + H_{dcp}^2 - R_d^2}{2 \times bc \times H_{dcp}}\right) \end{array} \right. \rightarrow \angle A_p = \angle c_1 + \angle c_2 + \angle A_c - \pi \quad (1)$$

$$\left\{ \begin{array}{l} \text{sine law} \rightarrow \angle b_1 = \sin^{-1}\left(\frac{H_{dcp}}{R_d} \sin \angle c_2\right) \\ \text{sine law} \rightarrow \angle b_2 = \sin^{-1}\left(\frac{R_c \cos A_{offc} \sin \angle c_1}{ab}\right) \end{array} \right. \rightarrow \angle A_d = 2\pi - (\angle b_1 + \angle b_2 + \text{tg}^{-1}\left(\frac{H_{dct}}{D_{dct}}\right)) \quad (2)$$

Similar formulas are used to calculate the angles of the connecting rods and the upper arm with X direction (see Equations 3 and 4) as depicted in Figure 2a:

$$ab \text{ should be converted to } af = \sqrt{H_{act}^2 + D_{act}^2} \quad , \quad \angle fag = \angle A_c - \left(\frac{\pi}{2} + \text{tg}^{-1}\left(\frac{D_{act}}{H_{act}}\right)\right)$$

$$bc \text{ should be converted to } fg = \sqrt{H_{act}^2 + D_{act}^2 + R_{c@b}^2 (\cos \angle A_{offc})^2 - 2\sqrt{H_{act}^2 + D_{act}^2} R_{c@b} (\cos \angle A_{offc}) \sin(\angle A_c - \text{tg}^{-1}\left(\frac{D_{act}}{H_{act}}\right))}$$

$R_c \cos \angle A_{offc}$, H_{dcp} and R_d should be converted to $R_{c@b} \cos \angle A_{offc}$, $L_b \cos \angle A_{offb}$ and $R_a \cos \angle A_{offa}$ respectively

$$\left\{ \begin{array}{l} \text{sine law} \rightarrow \angle g_1 = \sin^{-1}\left(\frac{af \cos(\angle A_c - \text{tg}^{-1}\left(\frac{D_{act}}{H_{act}}\right))}{fg}\right) \\ \text{cosine law} \rightarrow \angle g_2 = \cos^{-1}\left(\frac{fg^2 + (L_b \cos \angle A_{offb})^2 - (R_a \cos \angle A_{offa})^2}{2 \times fg \times L_b \cos \angle A_{offb}}\right) \end{array} \right. \rightarrow \angle A_b = \angle g_1 + \angle g_2 + \angle A_c - \pi \quad (3)$$

$$\left\{ \begin{array}{l} \text{sine law} \rightarrow \angle f_1 = \sin^{-1}\left(\frac{L_b \cos \angle A_{offb} \sin \angle g_2}{R_a \cos \angle A_{offa}}\right) \\ \text{sine law} \rightarrow \angle f_2 = \sin^{-1}\left(\frac{R_{c@b} \cos \angle A_{offc} \sin \angle g_1}{af}\right) \end{array} \right. \rightarrow \angle A_a = 2\pi - (\angle f_1 + \angle f_2 + \text{tg}^{-1}\left(\frac{H_{act}}{D_{act}}\right)) \quad (4)$$

Kinetics of three-point hitch mechanism of tractor during the plow penetration into the soil

In this paper, effect of transition of mounted chisel plow from operation to transport on longitudinal stability of tractor is expected, therefore a tractor that plows uphill is considered. In order to avoid lateral force of the plow, the plow is assumed to be symmetric. During penetration of the plow into the soil, the hydraulic system of tractor is in neutral mode i.e. the joint between tractor and plow can be considered as three point floating hitch, and the plow penetrates into the soil until the condition for the equilibrium of forces in Z direction is achieved. In other words, when the plow is above the ground surface, the component of the plow weight in Z direction, is completely supported by the three-point hitch mechanism, however when the stable depth of the plow is achieved, this component of the plow weight is neutralized by the normal force exerted on the plow from the ground. Therefore net component of the plow weight in Z direction that must be supported by the three-point hitch mechanism should be considered as a function of the depth ratio, which is defined as the ratio of the plow instantaneous depth to the plow set depth. In this paper linear function is used to define the relation between the components of the plow weight in Z and X directions and the plow depth ratio.

$$\text{depth ratio} = \frac{\text{instantaneous depth}}{\text{set depth}}$$

$$F_{zp} = m_p g (1 - |\text{depth ratio}|) \cos \angle A_g \quad (5)$$

$$F_{xp} = m_p g (1 - |\text{depth ratio}|) \sin \angle A_g \quad (6)$$

Draft resistance of the plow also depends on the plow instantaneous depth. Knowing the soil specific resistance (S_{sr}), the plow draft resistance can be calculated from Equation 7:

$$PR_{\text{penetration}} = S_{sr} \times W_p \times \text{instantaneous depth of plow} \quad (7)$$

F_{zp} and F_{xp} are applied to the center of gravity of plow, thus the torques of these forces about the axis that connects the lower hitch points of the mast of plow can be calculated. On the other hand, because the plow draft resistance is assumed to be applied to the center of that part of the plow that is penetrated into the soil, the torque of the plow draft resistance about the axis that connects the lower hitch points of the mast of plow can be calculated. Therefore F_d is obtained from the Equation 8 (see Figure 3):

$$\sum M_{c@p} = 0 \rightarrow F_d = \frac{F_{zp} D_{c.g.p} - F_{xp} H_{c.g.p} - PR \times H_{pr}}{H_{dcp} \cos(\angle A_p - \pi / 2) \cos(\angle A_d - \pi)} \quad (8)$$

where $H_{pr} = H_{cp} - \frac{\text{instantaneous depth}}{2}$

As shown in Figure 3, knowing F_d , equations of static equilibrium of forces in X and Z directions, yields the X and Z components of the forces of the lower arms as follows:

$$\sum F_x = 0 \rightarrow F_{cx} = PR + F_{xp} - F_d \cos(\angle A_d - \pi) \quad (9)$$

$$\sum F_z = 0 \rightarrow F_{cz} = F_{zp} - F_d \sin(\angle A_d - \pi) \quad (10)$$

According to the assumption that the plow is symmetric, each of the right and left lower arms supports half of the F_{cx} and F_{cz} i.e.

$$F_{cx \text{ righth}} = F_{cx \text{ lefth}} = \frac{F_{cx}}{2}, \quad F_{cz \text{ righth}} = F_{cz \text{ lefth}} = \frac{F_{cz}}{2}$$

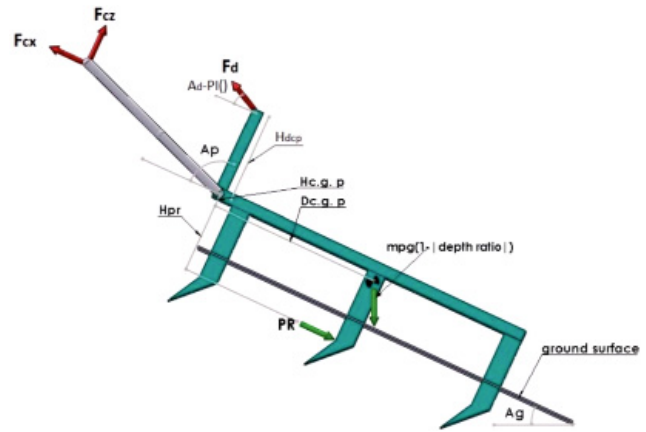


Figure 3. Free-body diagram of a mounted chisel plow during plow penetration into the soil

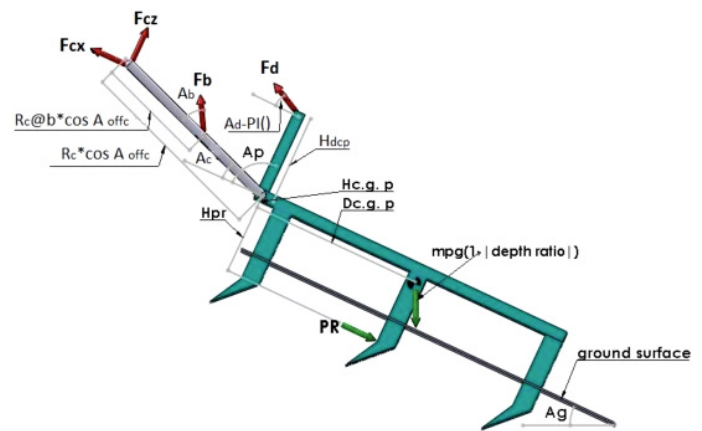


Figure 4. Free-body diagram of a mounted chisel plow during plow depth reduction

Kinetics of the three-point hitch mechanism during depth reduction of the plow

Depth of the mounted chisel plow is reduced due to the appearance of the forces in the connecting arms, i.e. the joint between tractor and plow can be considered as three point rigid hitch. These forces change the lower arms from bi- to tri-articulated beams. Therefore the effect of the connecting arm forces on the overall forces exerted on the tractor body must be considered. During depth reduction of the PR of the plow, the external forces of the plow, except the upper and the lower arms' forces; are F_{zp} , F_{xp} and PR. To exit the plow from the soil, component of the weight of plow plus the weight of the accumulated soil above the plow in Z direction must be overcome. Therefore F_{zp} was modeled as:

$$F_{zp} = (1 + K_1 (1 - \text{height ratio})) m_p g \cos \angle A_g \quad (11)$$

where K_1 determines the ratio of the weight of the accumulated soil to the plow weight and

$$\text{plow height ratio} = \frac{\text{instantaneous height of plow}}{\text{height of plow on the ground}} = (1 - |\text{depth ratio}|)$$

On the other hand, because during plow penetration into the soil, the plowshare is pushed to the plow furrow harder than during the plow depth reduction, the draft resistance of the plow is less in depth reduction phase than penetration. In the developed model PR is simulated as:

$$PR_{\text{depth reduction}} = K_2 S_{sp} W_p \times \text{instantaneous depth of plow} \quad (12)$$

$$\text{where } K_2 = \frac{\text{PR of plow in depth reduction phase}}{\text{PR of plow in penetration phase}}$$

During exit of the plow from the soil, plowshares are still surrounded by the soil, thus part of the component of the plow total weight in X direction is supported by the soil; therefore F_{xp} can be modeled as:

$$F_{xp} = (K_3 + (1 - K_3) \times \text{height ratio}) \times (m_p + m_s)g \times \sin \angle A_g \quad \text{where} \quad (13)$$

m_s = mass of the soil supported by the plow = $K_1(1 - \text{height ratio}) \times m_p g$ and

$$K_3 = \frac{\text{the component of the plow total weight in X direction when the plow is in the soil}}{\text{the component of the plow total weight in X direction when the plow is out of the soil}}$$

According to Figure 4, knowing F_{zp} , F_{xp} and PR, the force of the upper arm (F_{ua}), can be calculated using equation of the static equilibrium of torques about the axis that connects the lower hitch points of the plow mast (same as Equation 8)

To formulate F_b , equation of the static equilibrium of torques about the lower hitch points of the tractor is necessary. (see Figure 4)

$$\sum M_{c@t} = 0 \rightarrow F_b = \frac{[F_{zp}(D_{c.g.p} + R_c \cos \angle A_{offc} \sin \angle A_c) - PR(H_{pr} + R_c \cos \angle A_{offc} \sin \angle A_c) - F_{xp}(H_{c.g.p} + R_c \cos \angle A_{offc} \sin \angle A_c) - F_d \cos \angle A_d (H_{dcp} \cos(\angle A_p - \pi/2) - R_c \cos \angle A_{offc} \sin \angle A_c)]}{2 \cos \angle A_{offb} \sin \angle A_b \times R_{c@b} \cos \angle A_{offc}} \quad (14)$$

According to Figure 4, equations of the static equilibrium of forces in X and Z directions calculate the lower arm forces as follows:

$$\sum F_x = 0 \rightarrow F_{cx \text{ righth}} = F_{cx \text{ left}} = \frac{PR + F_{xp} - 2F_b \cos \angle A_{offb} \cos \angle A_b - P_d \cos \angle A_d}{2} \quad (15)$$

$$\sum F_z = 0 \rightarrow F_{cz \text{ righth}} = F_{cz \text{ left}} = \frac{F_{zp} - 2F_b \cos \angle A_{offb} \sin \angle A_b - P_d \sin \angle A_d}{2} \quad (16)$$

The torque exerted on the tractor body due to the forces of the connecting rods is calculated from Equation 17:

$$M_{F_b \text{ induced}} = \overline{R_a} \times 2\overline{F_b} = R_a \cos \angle A_{offa} \times 2F_b \sin(\angle A_a - \angle A_b) \times \cos \angle A_{offb} \quad (17)$$

Development of the longitudinal stability index of tractor ($TSI_{\text{longitudinal}}$)

The longitudinal stability index of a tractor that plows uphill is defined as the ratio of the dynamic load of the tractor front axle to the static load of it when the tractor is on level ground. Knowing the coordinates of the tractor center of gravity (c.g.), and the tractor weight, the static load of the tractor front axle on level ground can be calculated as:

$$\text{front axle static load on level ground} = \frac{WBr}{WB} \times m_t g \quad (18)$$

where WB and WBr are the wheel base of tractor and the horizontal distance between the tractor rear wheel axle and the center of gravity of tractor.

To formulate the equation of the front axle dynamic load, effects of the ground slope and the forces and torques exerted on the tractor from the three-point hitch mechanism must be considered. Therefore all of these forces and torques must be transferred to the center of gravity of tractor. Reaction force of the front axle when the tractor is located longitudinally on a slope is considered as the front axle dynamic load. If vectors

connecting the center of gravity of tractor to upper, right lower, left lower, right lift, and left lift arms of tractor are shown as $\overline{d_d}$, $\overline{d_{cr}}$, $\overline{d_{cl}}$, $\overline{d_{ar}}$ and $\overline{d_{al}}$ respectively, the transferred force and torque to the center of gravity of tractor can be calculated as:

$$\overline{F_{@c.g.t}} = \overline{m_t g} + \overline{F_d} + \overline{F_{cr}} + \overline{F_{cl}} + \overline{F_{ar}} + \overline{F_{al}} \quad (19)$$

$$\overline{M_{@c.g.t}} = \overline{M_{F_b \text{ induced}}} + (\overline{d_d} \times \overline{F_d}) + (\overline{d_{cr}} \times \overline{F_{cr}}) + (\overline{d_{cl}} \times \overline{F_{cl}}) + (\overline{d_{ar}} \times \overline{F_{ar}}) + (\overline{d_{al}} \times \overline{F_{al}}) \quad (20)$$

Because tractor travels along the slope and the plow is symmetric, forces applied in Y direction and torques exerted about X and Z axes neutralize each other. Thus total force and torque applied to the center of gravity of tractor can be simplified to $F_{X@c.g.t}$, $F_{Z@c.g.t}$ and $M_{@c.g.t}$ as depicted in Figure 5:

Equation of static equilibrium of torques about the hypothetical line connecting the wheel-ground contact points of tractor rear wheels yields the front axle dynamic load:

$$\sum M_{\text{tractor rear wheels contact points with ground}} = 0 \rightarrow \text{front axle dynamic load} = \frac{WBr F_{z@c.g.t} - H_{c.g.t} F_{x@c.g.t} - M_{@c.g.t}}{WB} \quad (21)$$

where $H_{c.g.t}$ is the height of the tractor c.g.

Finally, the formula for the longitudinal stability of tractor can be written as:

$$TSI_{\text{longitudinal}} = \frac{\text{front axle dynamic load}}{\text{front axle static load when tractor is on level ground}} = \frac{WBr F_{z@c.g.t} - H_{c.g.t} F_{x@c.g.t} - M_{@c.g.t}}{WBr \times m_t g} \quad (22)$$

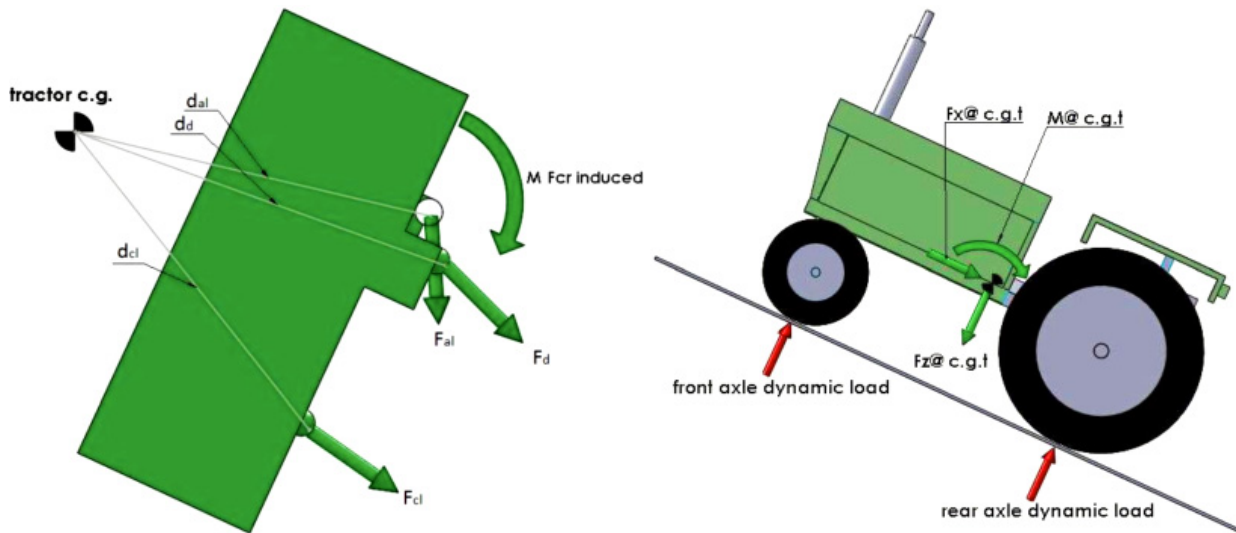


Figure 5. Forces and torque exerted on the hitch points of the three-point hitch mechanism of tractor (a), and the free-body diagram of the tractor that pulls a mounted chisel plow (b)

In order to simplify calculations of the derived formulas, spreadsheet software (Excel, Microsoft Corporation, Redmond, Wash.) was utilized. Test of the model was carried out with different geometries and mass specifications of tractor MF285 and chisel plow (which were measured from tractor-chisel plow combination) as the input parameters of the model. Finally related diagrams were drawn to depict the relation between some of the outputs of the model relative to their dependant parameters.

Results and discussion

Values of parameters considered as the inputs of the model are listed in Table 1:

In order to clarify the effect of the plow transition from operation to transport on the forces of the upper and lower arms, the force of the connecting rods and the angular position of the arms of the three-point hitch mechanism, related charts that display these variables according to the depth and height ratios were drawn with the aid of Excel software (as shown in Figure 6). In order to separate the plow penetration from the plow depth reduction phases of the charts, depth ratio was considered as a negative value between the range of [-100%, 0%], where the value of 0% is for the onset instant of the plow penetration into the

soil and the value of -100% is achieved when the plow reaches to its stable depth, and the height ratio was considered as a positive value between the range of [0%, 100%], where the value of 0% is for the onset instant of the plow depth reduction and the value of 100% is achieved when the plow reaches the soil surface.

Figure 6-a shows the effect of plow depth variations on the value of the internal force of the upper arm, Figure 6b depicts the effect of the plow depth variations on the values of the internal forces of the right lower arm in X and Z directions, and Figure 6c makes clear the effect of plow depth variations on the value of the internal force of the right connecting rod. As shown in Figure 6c, during the plow penetration into the soil, force of the right connecting rod is zero and positive values are obtained for the forces of the right connecting rod during depth reduction of the plow, therefore the connecting rods act only as pulling beams. This result of the model is in agreement with reality. On the other hand, an increase of the plow depth above the 20% of the plow stable depth, converts the upper arm of the tractor from pulling to pushing beam (Figure 6a). This result is comparable to the result obtained by Alimardani et al. (2008) that was about testing a three point hitch dynamometer. They stated that: "During plowing, top-link arm is subjected to compression while the lower links undergoes tensile forces". Therefore, it can

Table 1. Input parameters of the developed model

Parameter	Value	Unit	Parameter	Value	Unit	Parameter	Value	Unit
A_g	0.4	rad	H_{cp}	0.75	m	R_d	0.85	m
A_{offb}	0.06	rad	H_{dcp}	0.5	m	S_{sr}	44	kN/m ²
A_{offc}	0.14	rad	H_{dct}	0.35	m	WB	2.3	m
A_{offa}	0.1	rad	K_i	0.4	-	WBr	0.91	m
$D_{c.g.p}$	1	m	L_b	0.75	m	$X_{cr} \& X_{cl}$	-0.65	m
D_{act}	0.1	m	m_p	2.5	kN	$X_{ar} \& X_{al}$	-0.7	m
D_{dct}	0.15	m	m_t	28	kN	X_d	-0.75	m
$H_{c.g.p}$	0.5	m	R_c	1	m	$Z_{cr} \& Z_{cl}$	-0.2	m
$H_{c.g.t}$	0.85	m	$R_{c@b}$	0.55	m	$Z_{ar} \& Z_{al}$	0.5	m
H_{act}	0.45	m	R_a	0.3	m	Z_d	0.25	m

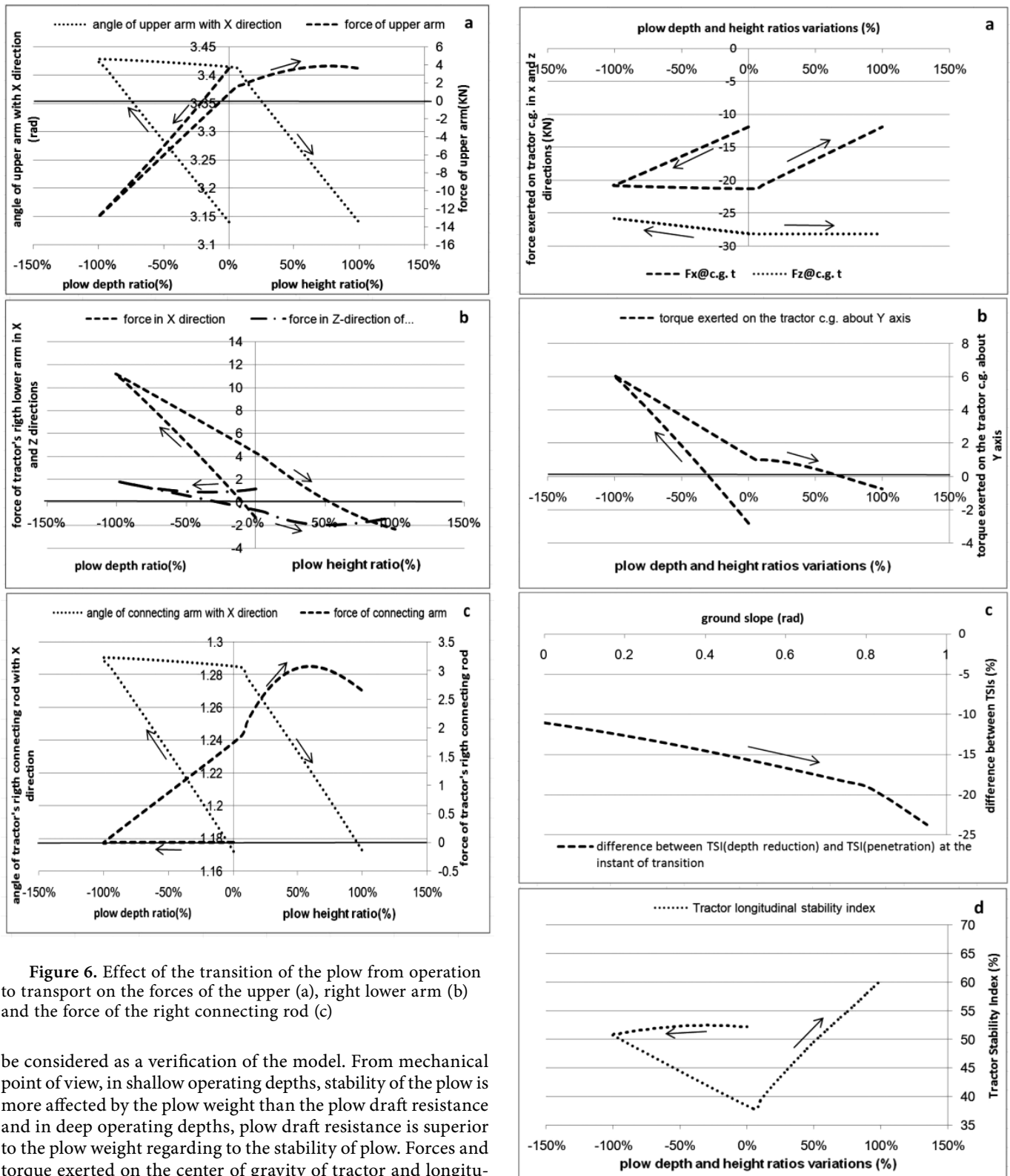


Figure 6. Effect of the transition of the plow from operation to transport on the forces of the upper (a), right lower arm (b) and the force of the right connecting rod (c)

be considered as a verification of the model. From mechanical point of view, in shallow operating depths, stability of the plow is more affected by the plow weight than the plow draft resistance and in deep operating depths, plow draft resistance is superior to the plow weight regarding to the stability of plow. Forces and torque exerted on the center of gravity of tractor and longitudinal stability index of tractor as a function of the plow depth and height ratios are charted in Figure 7. Effect of the ground slope on the reduction of the stability index at the moment of the transition of the plow from operation to transport is shown in Figure 7c, too.

Figure 7. Forces (a) and torque (b) exerted on the center of gravity of tractor, and longitudinal stability index of tractor (d) as a function of the plow depth and height ratios and the effect of the ground slope on the reduction of the stability index at the moment of the plow transition from operation to transport (c)

As shown in Figure 7a, when the plow depth increases, the model predicts the increase of the force exerted on the center of gravity of tractor in X direction. However the force exerted on the center of gravity of tractor in Z direction, is almost not affected by the plow depth and height ratio variations, and the value of this force in plow depth reduction is more than the plow penetration into the soil, because the weight of the soil accumulated above the plow adds to the plow weight during the plow depth reduction. This result of the model is in agreement with the results obtained by Abu Hamadeh and Al Jalil (2004), which was about theoretical simulation of a tractor-trailer system moving up and down sloping ground under different operating conditions. They found that the parallel component of the drawbar pull increased with the increase in slope angle and trailer loading, while the normal component of drawbar pull decreased slightly with the increase in slope angle and trailer loading. Since the increase of plowing depth in mounted implements is similar to increase of trailer loading and slope angle of trailed implements, similarity between the obtained results verifies that the assumptions of the model are rational. It should be noted from the Figure 7d that during the plow penetration into the soil, $TSI_{\text{longitudinal}}$ is almost constant, because the transferred load from the front axle to the rear axle resulted from the increase of the plow draft resistance during the plow penetration and its effect that is clear from the increase of force of the lower arm in X direction (Figure 6b); may be compensated by the transferred load from the rear axle to the front axle, that is resulted from the conversion of the upper arm from the pulling to pushing beam (Figure 6a). However at the instant of the plow transition from operation to transport, $TSI_{\text{longitudinal}}$ is reduced severely, in other words, at this moment, the tractor is susceptible to backward overturning. On the other hand, as can be seen from Figure 7c, in steeper slopes, the reduction of the $TSI_{\text{longitudinal}}$ at the instant of the plow transition from operation to transport increases. Therefore, in situation when the tractor works on steep slopes, plow transition from operation to transport should be avoided.

Conclusion

Simulation and modeling of a physical phenomenon is one of the cheapest methods utilized to predict the behavior of that phenomenon in response to the variation of its independent variables. Therefore it is suitable to model tractor and mounted implement combination in order to examine the effects of the transition of these implements from operation to transport on longitudinal stability of a tractor which works on sloping ground. In this study simulation of the combination of a tractor and a chisel plow in penetration and depth reduction phases of the plow was considered. The main results obtained from this study are as follows:

- 1 During the plow penetration into the soil value of force of the connecting rods was equal to zero.
- 2 During depth reduction of the plow the connecting rods acted only as pulling beams.
- 3 Increase of the plow depth above 20% of its stable depth converted the upper arm of the tractor from pulling to pushing beam.

- 4 Increase of the plow depth led to the increase of the force exerted on the center of gravity of tractor in X direction.
- 5 Plow depth and height ratio variations did not affect the value of force exerted on the center of gravity of tractor in Z direction.
- 6 During the plow penetration into the soil, the value of $TSI_{\text{longitudinal}}$ was approximately constant.
- 7 At the instant of the plow transition from operation to transport $TSI_{\text{longitudinal}}$ was reduced severely, in other words, at this moment; the tractor was susceptible to backward overturning.

Nomenclature

Item	Description	Unit
A_i	Angle of the component i with positive direction of X axis	rad
$A_{\text{off } i}$	Offset angle of the component i with X-Z plane	rad
c.g.p & c.g.t	Center of gravity of plow and tractor, respectively	
b	Connecting rod of the tractor	
D_{ijk}	Distance from component i to component j of tractor or plow (k) that is parallel to X axis	m
d_{ii}	Length between the center of gravity of tractor and the hitch point of the left arm i	m
$D_{\text{act}} \& H_{\text{act}}$	Distance from the lift arm to the lower arm of tractor in X and Z directions, respectively	m
$F_{ix} \& F_{iz}$	Force of the component i in X or Z directions, respectively	kN
$F_{x@c.g.t} \& F_{z@c.g.t}$	Force exerted on the center of gravity of tractor in X and Z directions, respectively	kN
H_{ijk}	Distance from component i to component j of tractor or plow (k) that is parallel to Z axis	m
H_{cp}	Height of the lower arm of the plow when the plow is on level ground	m
c	Lower arm of the tractor	
L_b	Length of the connecting rod	m
a	Lift arm of the tractor	
$M_{Fb \text{ induced}}$	Torque induced by F_b and exerted on the tractor body	kN.m
m_i	Mass of the object i	kg
p	Plow	
PR	Plow draft resistance	kN
R_i	Length of the tractor arm i that have a fixed point with tractor	m
$R_{c@b}$	Length of the lower arm up to the hitch point of the connecting rod	m
S_{sr}	Soil specific resistance	kN/m ²
t	Tractor	
d	Upper arm of the tractor	
dcp	Distance from upper arm to lower arm of the plow	m
dct	Distance from upper arm to lower arm of the tractor	m
W_i	Width of the object i	m

References

- Abu Hamadeh, N. H., Al Jalil H. F. (2004). Computer simulation of stability and control of tractor trailed implement combinations under different operating conditions. *Bragantia*, Campinas. 63: 149-162.
- Alimardani R., Fazel Z., Akram A., Mahmoudi A., Varnamkhasti, M.G. (2008). Design and Development of a three-point hitch dynamometer. *Journal of Agricultural Technology*. 4(1): 37 – 52.

- Liu J., Ayers P. D. (1999). Off-road vehicle rollover and filed testing of stability index. *J Agric Safety Health*. 5(1): 59–71.
- Liu J., Ayers P. D., Vance M. (1999). Off-road vehicle stability mapping integrating GPS/GIS and video technology. An ASAE meeting presentation.
- Mashadi B., Nasrolahi H. (2009). Automatic control of a modified tractor to work on steep side slopes. *Journal of Terramechanics*. 46: 299–311.
- Pota H., Katupitiya, J., Eaton R. (2007). Simulation of a tractor-implement model under the influence of lateral disturbances. *Proceedings of the 46th IEEE Conference on Decision and Control*. New Orleans, LA, USA, Dec. 12-14.
- Silleli H., Dayiog M. A., Ltekinb A., Ekmekc K., Yildızb M. A., Akayb E., Saranlı G. (2007). Anchor mechanism to increase the operator clearance zone on narrow-track wheeled agricultural tractors: prototype and first tests. *Biosystems Engineering*. 97: 153–161.
- Yisa M. G., Terao H. (1995). Dynamics of Tractor-implement Combinations on Slopes (Part I). *Journal of the Faculty of Agriculture*. Hokkaido University. 66(2): 240-262.

acs78_60